Research Report

2005-07

Impact of Inductor Placement on the Performance of Adjustable Speed Drives Under Input Voltage Unbalance and Sag Conditions

Lee, K., T. M. Jahns*, D. W. Novotny*, T. A. Lipo*, W. E. Berkopec**, V. Blasko#**

**Eaton Corp
4201North 27th St.
Milwaukee, WI 53216

*University of Wisconsin-Madison
1415 Engineering Dr.
Madison, WI 53706

#Otis Elevator Co.
Five Farm Springs Rd.
Farmington, CT 06032

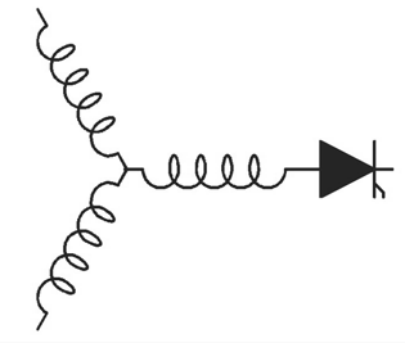

Wisconsin
Electric
Machines &
Power
Electronics
Consortium

University of Wisconsin-Madison
College of Engineering
Wisconsin Power Electronics Research Center
2559D Engineering Hall
1415 Engineering Drive
Madison, WI 53706-1691

© 2005 Confidential

IEEE 2005 International Electric Machines and Drives Conference (IEMDC'05)
San Antonio, TX USA, May 15-18, 2005

Impact of Inductor Placement on the Performance of Adjustable Speed Drives Under Input Voltage Unbalance and Sag Conditions

Kevin Lee[†] Thomas M. Jahns* D.W. Novotny* Thomas A. Lipo* William E. Berkopec[†] Vladmir Blasko[#]

[†] Eaton Corp.
4201 North 27th St.
Milwaukee, WI 53216

[*] University of Wisconsin – Madison
1415 Engineering Dr.
Madison, WI 53706

[#] Otis Elevator Co.
Five Farm Springs Rd.
Farmington, CT 06032

***Abstract* - Voltage unbalance or sag conditions generated by the line excitation can cause the input rectifier stage of an adjustable-speed drive (ASD) to enter single-phase rectifier operation. This degradation of the input power quality can have a significant negative impact on the induction machine performance characteristics, but the presence of an *LC* filter in the drive's input rectifier stage can be used to attenuate these undesired effects. The purpose of this paper is to investigate the impact of the inductor placement in the ASD topology on the drive's performance under voltage unbalance or sag conditions. More specifically, the relative advantages of choosing either a dc link choke inductor or three ac line inductors are discussed using a combination of closed-form analysis and simulations. The results of first-order sizing calculations show that a dc link choke inductor may offer some volume and mass advantages over three separate ac line inductors for the same ASD performance under unbalanced voltage conditions. Experimental results using a 5 hp ASD confirm the key analytical performance predictions.**

I. INTRODUCTION

Power quality problems and survey results have been reported in many publications [1, 2, 3]. The affected industry and businesses include automobile manufacturing plants, medical centers, semiconductor manufacturing plants, broadcasting facilities, and industrial and commercial buildings. It is estimated that industrial and digital economy companies collectively lose $45.7 billion a year to outages and another $6.7 billion each year to power quality phenomena [4]. Among various power quality disturbances, voltage sags have the most frequent occurrences [5].

The most frequent source of voltage sags is a transient current increase that persists between one cycle and a few seconds [6]. Such current transients may be caused by a variety of electrical phenomena including motor starting, transformer energization, short-circuit faults, and fast re-closing of circuit breakers [7]. Even though voltage sags are transient events, steady-state voltage unbalance can also exist caused by a variety of sources including unbalanced loads on the utility lines upstream from the ASD load [8].

Input voltage unbalance and sag conditions can have serious performance consequences in ASDs, including abnormally low input line power factor, high input current harmonic distortion, overstressed dc bus capacitors, high pulsating torque, and motor overheating. In the U.S. today, the overall cost of motor life loss due to harmonic pollution and voltage imbalance is estimated to be US$1 to 2 billion per year [9].

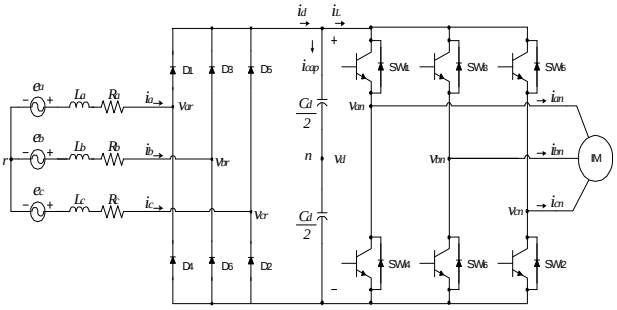

Figure 1: Induction machine ASD power circuit diagram including three identical input line inductors L_a, L_b, and L_c.

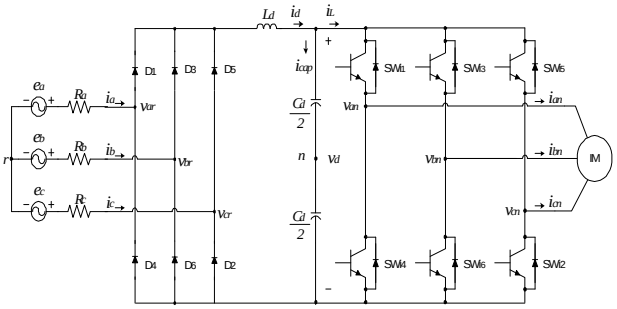

Figure 2: Induction machine ASD power circuit diagram including a dc link choke inductor L_d.

Attention in this paper is focused on general-purpose ASDs that consist of a three-phase rectifier input stage, a dc link, and a PWM inverter stage that delivers constant Volts-per-Hertz excitation to an induction motor. Voltage sag or unbalance conditions at the ASD line inputs can cause the rectifier stage to transfer into single-phase rectifier operation, creating significant amounts of harmonic voltage at twice the line frequency (120 Hz for 60 Hz excitation) on the dc link. This voltage ripple at the inverter input terminals has a degrading effect on the PWM output voltage waveforms, causing undesired low-frequency harmonic currents to flow in the machine. The resulting pulsating torque can cause significant degradation of the ASD performance in the forms of acoustic noise and mechanical vibrations. The vibration problem will be particularly severe if one of the torque harmonic frequencies falls close to a natural frequency of the mechanical driveline.

A previous paper has analyzed the performance effects of voltage sag and imbalance conditions when ac line inductors are used to filter the current in combination with capacitors on

the dc link [10]. The power stage schematic diagram of this popular ASD configuration is shown in Fig. 1. However, an important variant of this power circuit topology replaces the three ac line filter inductors in Fig. 1 with a single dc link choke inductor as shown in Fig. 2. The question immediately arises about which of these two configurations is better for attenuating the power quality problems induced by the voltage sags or unbalance at minimum mass, volume, and cost.

The purpose of this paper includes the following two objectives: 1) expansion of the previous analytical investigation to include the effects of a dc link choke inductor on ASD-driven induction machine performances under input voltage unbalance/sag conditions; and 2) comparison of the ASD voltage unbalance/sag performance when only a dc link choke inductor or ac line inductors are used. Attention is focused on the generation of harmonic current and pulsating torque in the induction machine in response to the second line harmonic frequency component that appears in the dc link voltage since it dominates the resulting harmonic effects.

The closed-form analytical expressions are verified using a combination of dynamic simulations and experimental tests. A 5 hp, 460 V ASD system is used as the target for these experimental verification efforts, providing valuable results that raise confidence in the accuracy and value of the analytical results. The availability of these analytical and experimental verification results makes it possible to investigate size and weight comparisons between the line inductor and dc choke inductor configurations for comparable input power quality performance.

II. Classification of Voltage Unbalance and Sags

Results from different power quality surveys generally indicate that the most common voltage sags in three-phase power systems are Types A, C and D [1]. The voltages in all the three phases drop in magnitude by the same amount for Type A voltage sags. On the other hand, voltages are affected differently in the three phases with either a Type C or D sag.

Figure 3 illustrates the typical three-phase voltage phasors under unbalanced conditions for Types C and D sags. This paper focuses on the effects of Type C voltage sags on the operation of a three-phase rectifier, although the analytical method presented herein can be extended to study the effect of Type D sags as well. The Type C sag was chosen because it is relatively common among voltage sag events and causes the rectifier to transfer into single-phase conduction quite easily.

Although the classification based on the type of sag is useful in studying their effects on circuits, it is common to quantify the amount of imbalance on the basis of percentages. Applying the IEEE definition of phase-voltage unbalance in three-phase systems [11], the voltage unbalance can be quantified using the following definitions:

$$unbalance\% = \frac{|V_{avg} - V_{\Phi}|}{V_{avg}} \quad (1)$$

$$V_{avg} = \frac{V_a + V_b + V_c}{3} \quad \text{[Vrms]} \quad (2)$$

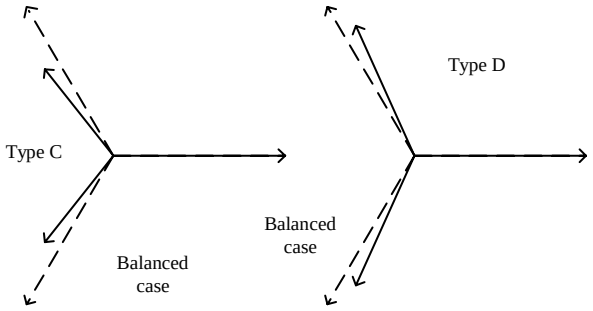

Figure 3. Phasor diagrams of Type C and D three-phase voltage unbalances

where V_{Φ} is the amplitude of the input phase voltage (either V_a, V_b, or V_c) that produces the largest deviation from the average voltage defined in (2).

Having defined the particular type of sag to be studied along with a preferred metric for the amplitude of the sag, the techniques for analyzing the ASD systems in the presence of such sags are presented in the following section.

III. ASD System Analysis

For the ASD configurations that are the subject of this investigation (Figs. 1 and 2), three-phase ac line voltages are fed to a three-phase rectifier (D_1-D_6) bridge. The input line impedance values in Fig. 1 and 2 are assumed to be equal (i.e., balanced), consisting of resistance R_a and line inductance L_a (ie., $L_a = L_b = L_c$ for Fig. 1). The dc bus voltage is buffered by dc bus capacitance C_d. These line inductors are eliminated in Fig. 2 in favor of a single dc link inductor. The PWM inverter consists of six IGBT switches (SW_1- SW_6) and their anti-parallel diodes. PWM control of these switches is used to synthesize variable-frequency, variable-amplitude ac voltage waveforms that are delivered to the induction machine following a constant Volts-per-Hertz algorithm.

It has been shown previously [12] that the input rectifier stage of the ASD configuration using ac line inductors (Fig. 1) can easily slip into single-phase operation during input voltage sag or unbalance conditions. The dominant ac component in the resulting bus voltage V_d waveform occurs at the second line harmonic frequency (120 Hz). It is this second harmonic voltage component that, in turn, dominates the generation of undesirable line sag/unbalance effects in the induction machine operating characteristics.

Analysis of the ASD configuration using a dc link choke inductor (Fig. 2) reveals that this topology behaves almost identically to the line inductor configuration during Type C unbalance conditions. That is, the ASD with the dc link inductor is vulnerable to entering single-phase operation of the input rectifier stage with only a modest amount of voltage unbalance, just as in the case with ac line inductors. Provided that the rectifier current is discontinuous so that there is no current flowing when the single-phase input voltage changes polarity, there will be no rectifier commutation effects. Under these conditions, the rectifier output voltage waveform will be identical in both cases.

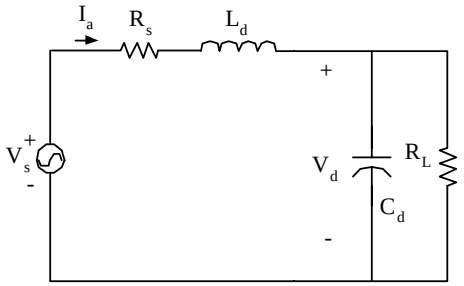

Figure 4. Equivalent circuit during single-phase operation.

The equivalent circuit of the ASD input stage with the dc link inductor under such single-phase excitation conditions is almost identical to the corresponding circuit for the ASD with line inductors [12]. As shown in Fig. 4, the only difference is that the inductance that appears in the *RLC* circuit consists of a single link inductor L_d instead of two line inductors L_a in series. The resistance R_L that appears in this circuit is the simplified representation of the inverter and motor load.

The closed-form solution of the second-order *RLC* circuit in Fig. 4 leads to the following time-domain expression for the dc bus voltage $V_d(t)$:

$$V_d(t) = \begin{cases} A \cdot e^{-\alpha t} \cdot \cos(\beta t) + B \cdot e^{-\alpha t} \cdot \sin(\beta t) + M \cdot \cos(\omega t) \\ \quad + N \cdot \sin(\omega t) & t_{in} < t < t_{ex} \\ V_d(t_{ex}) \cdot e^{-\frac{t - t_{ex}}{C_{dc} R_L}} & t_{ex} < t < t_{in} + \frac{T}{2} \end{cases} \quad (3)$$

where t_{in} is the bus current i_d inception time, t_{ex} is the extinction time, and T is the period of the ac excitation frequency (e.g., 1/60 = 16.7 ms for 60 Hz excitation).

All of the other coefficient definitions and derivation details for (3) are provided in a separate paper [12], with the added stipulation that inductance L_s has the following values for the two ASD configurations:

$$L_s = 2\,L_a \quad \text{for ASD with line inductors (Fig. 1)} \quad (4)$$

$$L_s = L_d \quad \text{for ASD with dc link inductor (Fig. 2)} \quad (5)$$

This closed-form bus voltage expression makes it possible to analyze and compare the effects of finite values of input line inductance or dc link inductance on induction machine performance during sag/unbalance conditions.

Closed-form solutions have also been developed for the induction machine currents and torque in the presence of dc link voltage variations expressed in (3). Here again, the interested reader is referred to [12] where the derivations are presented and discussed in more detail.

Only the major attributes of the resulting closed-form solution for the machine variables are summarized here. The dominant ac frequency component that appears in the dc link voltage during the single-phase operating mode falls at twice the excitation frequency ($2\omega_i$). As a result, the dc bus voltage $V_d(t)$ in (3) can be approximated as:

$$V_d(t) = V_{dc} + V_{dc2} \cdot \cos(2\omega_i t + \theta_2) \quad (6)$$

where V_{dc} is the average value of the dc bus voltage, V_{dc2} is the amplitude of the 2nd-harmonic voltage component, and θ_2 is the corresponding phase angle.

The effect of the inverter PWM operation is to produce machine phase voltages and currents that contain three major frequency components: a steady-state component at the inverter fundamental output frequency ω_0, a sum-frequency component at $2\omega_i + \omega_0$, and a difference-frequency component at $2\omega_i - \omega_0$. These latter two components are caused by the single-phase rectifier operation and are undesired.

More specifically, the closed-form expression for the phase *a* current that results from the closed-form analysis has the following form:

$$I_a(t) = I_{so}\cos(\omega_o t + \varphi_o) + I_{s1}\cos((2\omega_i + \omega_o)t + \varphi_1) + \\ + I_{s2}\cos((2\omega_i - \omega_o)t + \varphi_2) \quad (7)$$

while the instantaneous machine torque can be expressed as:

$$T_e = T_{e0} + T_{e2}\cos(2\omega_i t + \phi_2) + T_{e4}\cos(4\omega_i t + \phi_4) \quad (8)$$

It should be noted that the torque expression in (8) includes an average dc term that is contributed by the balanced three-phase excitation, and pulsating torque components at twice and four times the line frequency that appear because of the input voltage unbalance.

IV. Performance Comparisons with Line and DC Link Inductors

A key result of the closed-form analysis is that an ASD with line inductors (Fig. 1) that each have a value L_a should have identical performance during unbalanced single-phase operation as an ASD with a dc link inductor (Fig. 2) that has a value $2L_a$.

Since the closed-loop analysis necessarily requires several simplifications and approximations, it is desirable to determine whether this key equivalency result can be confirmed using more detailed models of the nonlinear ASD configurations. To accomplish this objective, the drive systems in Figs. 1 and 2 were first subjected to closed-form analysis and then simulated using Simplorer. This exercise has the dual benefits of comparing the closed-form and simulation results, as well as comparing the results for the two ASD configurations during unbalanced operation.

The simulation includes explicit models of the diode rectifier stage and space-vector PWM operation of the inverter stage so that it captures the effects of higher-order harmonics in the dc bus voltage under input line sag/unbalance conditions (i.e., beyond 2nd line harmonic) that are neglected in the closed-form analysis. The parameters of the 5 hp, 460 V induction machine are provided in [10].

The two ASD drive configurations are identical in almost all regards except for the inductors. Both are 5 hp, 460V drive systems with the same inverter load (L_{out} = 1.5 mH in series with each machine phase, 50% load), the same shared power converter component values (C_d = 330 μF, R_s = 0.01 Ω), and

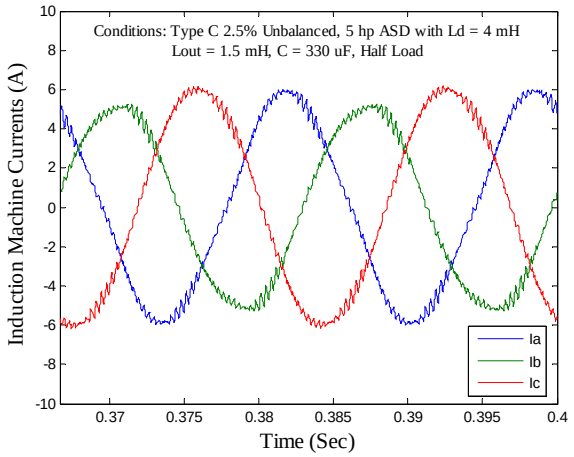

Figure 5: Simulation results of machine phase currents during Type C sag with 2.5% voltage unbalance (50% load) with dc link choke inductor.

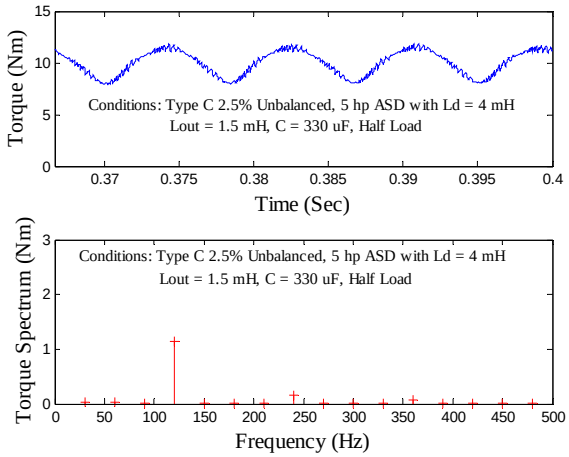

Figure 6: Simulation results of machine torque frequency spectrum during Type C sag with 2.5% voltage unbalance (50% load) with dc link choke inductor.

the same unbalanced excitation conditions (Type C sag, 2.5% unbalance). For the Fig. 1 ASD configuration, the value of each ac line inductor is 2 mH, while the value of the dc link inductor in the Fig. 2 ASD configuration is 4 mH, meeting the equivalency conditions expressed in (4) and (5).

Since the results of the closed-form analysis and their comparison with simulation results have been thoroughly discussed elsewhere [10,12], only a couple results are presented here. It should be noted that the closed-form analysis results for the two ASD configurations must be exactly the same because the inductor values meet the required equivalency conditions, making the defining equations identical.

Figures 5 and 6 show the simulated induction machine stator currents and torque waveforms during unbalanced excitation conditions as described above for the ASD configuration in Fig. 2 with a dc link inductor. The effects of the 2.5% input voltage unbalance are quite apparent in all of these waveforms. Figure 6 also includes a frequency spectrum of the instantaneous torque waveform, confirming that the pulsating torque waveform is dominated by the frequency component at twice the input excitation frequency.

TABLE I. CLOSED FORM AND SIMULATED PULSATING TORQUE COMPARISON BETWEEN LINE INDUCTOR AND DC BUS CHOKE.

Conditions: 5 hp ASD at 50% Load with a Type C Sag at 2.5% Unbalance

Conditions: Type C, 2.5% Unb. 50% load	*Closed-Form Peak-to-Peak Pulsating Torque [Nm]*	*Simulated Peak-to-Peak Pulsating Torque [Nm]*
2 mH line inductor	3.38	3.28
4 mH link inductor	3.38	3.21

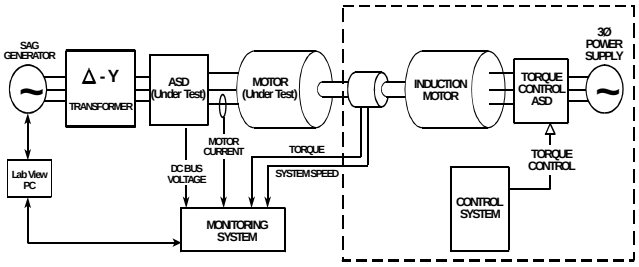

Figure 7: Experimental test equipment configuration.

Table I presents some important results comparing the predicted pulsating torque amplitudes for the closed-form and simulation analysis of the 2.5% Type C unbalance case in both ASD configurations. The agreement between the closed-form and simulation predictions for the peak-to-peak pulsating torque is quite good for each of the two ASD configurations.

In addition, the comparison between the simulation predictions of the peak-to-peak pulsating torque amplitude for the two ASD configurations is important. Since these two predictions agree very closely (within 1% of the average torque value of 10 Nm for this operating condition), the proposed equivalency condition expressed by $L_d = 2\ L_a$ based on the closed-form analysis is supported by the more detailed simulation results.

V. EXPERIMENTAL RESULTS

Experimental tests have been carried out using a 5 hp, 460 V, 60 Hz ASD mounted on a laboratory dynamometer. The ASD for this test has the Fig. 2 configuration with a dc link inductor. The test bed configuration is illustrated in Fig. 7, consisting of a programmable voltage sag generator, a drive isolation transformer, the ASD under test, an induction machine, a load machine excited by a four-quadrant ASD, and a Labview-based computer system designed to provide data acquisition, monitoring, and control functions.

The component values in the test power converter differ somewhat from those used in the preceding simulations in Section IV. For the test inverter, the value of the bus capacitance C_d is reduced from 330 μF to 235 μF, and the dc link inductor value is reduced from 4 mH to 3.22 mH. All of the other key system parameters and test conditions are the same as those presented in the preceding section.

Figure 8 provides a sample of the measured stator current waveforms for unbalanced (Type C sag) input voltage excitation conditions. Despite the differences in test conditions and the presence of the additional measurement noise, the similarities between the features of these current

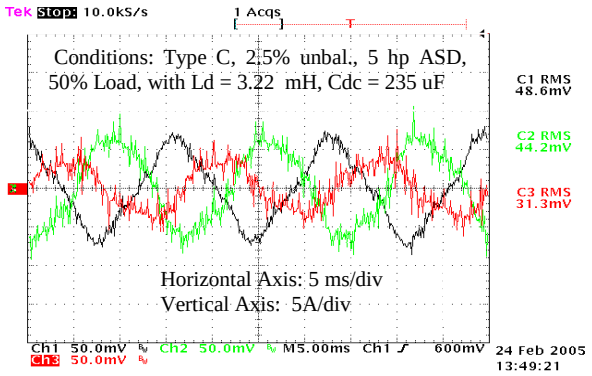

Figure 8: Measured stator current waveforms during Type C sag with 2.5% voltage unbalance (50% load) with dc bus choke.

TABLE II.
PULSATING TORQUE COMPARISON BETWEEN CLOSED-FORM ANALYSIS, SIMULATION, AND EXPERIMENTAL RESULTS FOR ASD WITH DC BUS CHOKE INDUCTOR

Conditions: 5 hp ASD at 50% Load with Type C Sag at 2.5% Unbalance

	Peak-to-Peak Pulsating Torque (Nm)	*Percentage of Average Torque*
Closed-Form	4.98	49.8%
Simulation	5.02	50.2%
Experiment	5.06	50.6 %

waveforms and the earlier simulated current waveforms in Fig. 5 are apparent.

Table II compares the measured peak-to-peak pulsating torque amplitude with the predicted values from the closed-form analysis and the simulation for the ASD configuration with the dc link inductor (Fig. 2). The peak-to-peak pulsating torque was measured using an in-line torquemeter with sufficient bandwidth to capture the low-frequency (i.e., 120 Hz) harmonic amplitude. The same test conditions of 50% rated load and Type C sag conditions with 2.5% voltage unbalance were applied in all three cases. The agreement between the pulsating torque amplitude derived from the closed-form analysis, the simulation, and experimental tests is quite good.

The torque ripple of the dc choke case is elevated in this case compared to the values in Table I because of the lower bus capacitance and dc line inductor values in the tested power converter compared to the values used in the Table I calculations.

Such comparisons provide evidence that the closed-form expressions presented in this paper can be applied to develop useful estimates of the impact of unbalanced excitation on induction machine performance.

VI. INDUCTOR RATINGS AND COMPARATIVE SIZING

It has been established in Section IV that the value of the dc link choke inductor should be twice that of each ac line inductor in order for the ASD configurations in Figs. 1 and 2 to deliver the same performance under unbalanced voltage conditions, assuming that all of the other component values are the same in both circuits. This section discusses the impact of the voltage unbalance on the inductor ratings and sizes. In addition, the relative sizes of the dc link choke inductor and combined three ac link inductors are discussed in order to gain some insights into their comparative masses, volumes, and materials costs.

Inductor Ratings

When voltage unbalance conditions occur that cause the ASD rectifier to transfer into single-phase operation, the loading on the inductors increases substantially if the motor load is unchanged. More specifically, the rectifier's transfer from balanced three-phase to single-phase operation causes the average dc link voltage to drop to 2/3^{rds} of its previous value. This means that the rms current rating of each inductor in either the Fig. 1 or Fig. 2 ASD configuration must increase by at least 50% compared to its balanced excitation rating in order to deliver the same power to the motor load.

Alternatively, the ASD output power can be reduced to approx. 2/3rd of its normal rating in order to reduce the inductor current back within its steady-state limits. The higher currents in the inductors will not pose a thermal problem for short voltage sags because of the long thermal time constants of the inductors. However, the elevated currents create difficulties if they cause the inductor magnetic core to enter saturation.

In addition to the higher current loads, unbalanced voltage excitation also causes additional core losses in the inductors for both ASD configurations. For example, the presence of line voltage sag and unbalance conditions causes the dc link choke inductor to be exposed to 120 Hz and its harmonics in addition to the 360 Hz components it experiences under normal balanced operating conditions. Table III captures the largest measured voltage harmonics that appear across the dc bus choke inductor used in this study. It should be noted that the 120 Hz and 240 Hz voltage components do not exist in balanced excitation case, while the 360 Hz component remains the same in both balanced the balanced and unbalanced cases. Similar arguments apply to increased core losses in the ac line inductors during unbalanced voltage operation.

TABLE III. MEASURED VOLTAGE ACROSS THE DC BUS CHOKE.

Conditions: 5 hp ASD at 50% Load with Type C Sag at 2.5% Unbalance

DC Choke 3.22 mH, 9 A	*120 Hz Component*	*240 Hz Component*	*360 Hz Component*
Voltage	9.3 V	3.5 V	21.3 V

Comparative Inductor Sizing

Although detailed sizing of the inductors in the two ASD configurations falls beyond the scope of this paper, a first-order comparison can be developed that provides useful insights into their relative volumes. The approach taken here is based on a well-known approach to inductor and transformer sizing that uses the product of the magnetic core cross-sectional area A_c and the winding window area A_w [13]. Although not exact, this A_cA_w area product can be used as a first-order metric that is monotonically related to the inductor

volume and mass. That is, the relative area product values for the dc link choke inductor and the line inductors (combined) can be used as an approximate measure of their relative sizes (volume or mass).

As a first step, the following condition based on equal magnetomotive forces (mmf) must be met in order for the dc link choke inductor and an ac line inductor to have the same maximum magnetic flux density levels:

$$\frac{N_{ac} I_{ac-pk}}{g_{ac}} = \frac{N_{dc} I_{dc-pk}}{g_{dc}} \tag{9}$$

where N_{ac} is the ac line inductor turns, N_{dc} is the dc choke inductor turns, I_{ac-pk} is the ac inductor peak current [A], I_{dc-pk} is the dc choke peak current (including ripple components) [A], g_{ac} is the ac line inductor air gap [m], and g_{dc} is the dc choke inductor air gap [m]. Since the current in the dc link choke inductor is exactly the rectified version of the ac line inductor current for single-phase operation, the peak currents in the two inductors are exactly equal (i.e, $I_{ac-pk} = I_{dc-pk}$).

Rearranging (9) and using the observation about peak current equality leads to:

$$\frac{N_{ac} g_{dc}}{N_{dc} g_{ac}} = \frac{I_{dc-pk}}{I_{ac-pk}} = 1 \tag{10}$$

The basic equation for inductance L can be expressed by:

$$L = \frac{\mu_o N^2 A_c}{g} \tag{11}$$

where N is the number of winding turns, g is the air gap length [m], and μ_o is the permeability of air.

Substituting in the corresponding quantities for the ac line inductor and dc choke inductor, the inductance ratio can be expressed as:

$$\frac{L_{ac}}{L_{dc}} = \frac{N_{ac}^2 A_{ac}}{N_{dc}^2 A_{dc}} \frac{g_{dc}}{g_{ac}} \tag{12}$$

where L_{ac} is the value of the ac line inductor inductance [H], L_{dc} is the corresponding value of the dc choke inductance [H], A_{ac} is the effective cross-sectional area of the ac line inductor core [m^2], and A_{dc} is the corresponding effective cross-sectional area of the dc link choke inductor core [m^2].

Combining (10) and (12) and rearranging, the ratio of the core cross-sectional areas for the two inductors is:

$$\frac{A_{ac}}{A_{dc}} = \frac{L_{ac}}{L_{dc}} \frac{N_{dc}}{N_{ac}} \tag{13}$$

Next, the conductor current density J [in Arms/m^2] is calculated as:

$$J = \frac{I}{A_{cond}} \tag{14}$$

where I is the rms conductor current [Arms] and A_{cond} is cross-sectional area of a single conductor.

If the inductor uses a total of N turns, the total winding window area can be approximated as A_w, calculated as follows, using (14):

$$A_w = N A_{cond} = N \frac{I}{J} \tag{15}$$

It should be noted that this simplified expression assumes 100% slot fill factor. However, since only ratios are being calculated, no error is introduced as long as the same 100% fill factor is assumed for both inductors.

The inductor comparison will be made assuming the same current density value J in both inductors. As a result, the ratio of the total window areas occupied by the conductors in the two inductors can be calculated using (15) as:

$$\frac{A_{wac}}{A_{wdc}} = \frac{N_{ac}}{N_{dc}} \frac{I_{ac-rms}}{I_{dc-rms}} \tag{16}$$

where A_{wac} is ac line inductor winding area, A_{wdc} is the dc link choke inductor winding area, and I_{ac-rms} and I_{dc-rms} are the rms currents in the ac line inductor and the dc link choke inductor, respectively. However, as pointed out above, the dc link inductor current is exactly the rectified version of the ac line inductor current in this case, meaning that the two rms current amplitudes must be exactly equal (i.e., $I_{ac-rms} = I_{dc-rms}$). As a result, (16) can be simplified as:

$$\frac{A_{wac}}{A_{wdc}} = \frac{N_{ac}}{N_{dc}} \tag{17}$$

Now, multiplying the core area and the window area ratio expressions in (13) and (17), the ratio of the core-window area products for the ac line inductor and the dc link choke inductor can be expressed very compactly as:

$$\frac{A_{wac} A_{ac}}{A_{wdc} A_{dc}} = \frac{N_{ac}}{N_{dc}} \frac{L_{ac}}{L_{dc}} \frac{N_{dc}}{N_{ac}} = \frac{L_{ac}}{L_{dc}} \tag{18}$$

Since the Fig. 1 ASD configuration requires three line inductors, the core-window area product ratio in (18) will be multiplied by 3 to compare the combined core-winding area product of the three line inductors to that of the single dc link choke inductor. At the same time, the relationship $L_{dc} = 2\, L_{ac}$ will be substituted in (18) in order to make the comparison on the basis of the same performance under unbalanced voltage conditions.

Thus, the core-winding product area of the combined three-phase line inductors is compared to that of the dc link choke inductor as:

$$\frac{3 A_{wac} A_{ac}}{A_{wdc} A_{dc}} = \frac{3 L_{ac}}{L_{dc}} = \frac{3}{2} \tag{19}$$

It would be too much of an oversimplification to equate this ratio of core-window areas in (19) to either the volume or mass ratios of inductors in the two ASD configurations. However, the result does suggest that the total volume and mass of the three ac line inductors may be larger than that of the dc link choke inductor for the same unbalanced voltage performance.

There are additional design factors that affect the inductor volumes and masses that make it necessary to cautiously evaluate this conclusion. For example, the sizing calculations presented above assume that the ac link inductors are each independent units. However, it is rather common to design 3-phase line inductors using a common magnetic core in order to save iron mass and volume. This approach would reduce and perhaps eliminate any volume or mass advantage that the dc link choke inductor would have over the ac line inductor approach.

Selection of ASD Inductor Configuration

There are many ASD design issues beyond voltage unbalance that influence the decision about whether to adopt ac line inductors (Fig. 1) or a dc link choke inductor (Fig. 2). For example, the dc link choke inductor configuration can be modified to help suppress conducted common-mode EMI by splitting the inductor into two equal parts mounted in series with the positive and negative dc link buses in Fig. 2. On the other hand, ac line inductors can be helpful in protecting the rectifier components from unexpected transient voltage spikes on the input lines.

Many other engineering issues including physical packaging and cooling will also influence the choice between the inductor configurations, as well as product marketing issues. Inductor performance under voltage unbalance conditions has not typically been a major influence on this decision, but this discussion has provided some insights about how this significant issue can be considered in future design exercises.

VII. CONCLUSIONS

This paper has explored the effects of a dc bus choke inductor on induction machine ASD performance during voltage unbalance/sag conditions. In addition, a useful evaluation of these effects is presented that compares ASDs using ac line inductors or a dc link choke inductor.

Analytical, simulation, and experimental results for the induction machine have been included in this paper for the ASD configurations with a dc bus choke inductor. Closed-form solutions for the resulting rectifier stage waveforms are derived to illustrate how input line voltage unbalance gives rise to dc bus voltage ripple that is dominated by the 2nd harmonic of the input line frequency (i.e., 120 Hz).

It has been shown that the performance of the two ASD configurations are almost identical if the inductance of the dc bus choke inductor is twice the value of each line inductor. For each of the two ASD configurations, the match between analytical, simulation and experimental results is very good.

Results of a comparative inductor sizing exercise show that the dc bus choke inductor configuration may offer some net mass and volume advantages over the ac line inductor configuration for achieving the same performance characteristics during voltage unbalance or sag conditions. However, practical inductor design and manufacturing issues may serve to minimize these differences in real ASD systems. In both ASD configurations, the transfer of the rectifier into single-phase operation due to the sudden appearance of unbalanced voltages will cause elevated current loads and core losses in the inductors if the motor load is not reduced.

This investigation has provided detailed information about the effects of voltage unbalance and sag conditions on ASD performance and the additional stresses placed on the drive circuit inductors. The authors hope that this information will be useful to engineers in determining the impact of unbalanced voltage conditions on future ASD designs as well as suggesting techniques for minimizing the negative effects on drive rating and performance.

REFERENCES

[1] M. H. J. Bollen, *Understanding power quality problems – voltages and interruptions*, New York: IEEE Press, 1999.

[2] D. O. Koval, R. A. Bocancea, K, Yao and M. B. Hughes, "Canadian national power quality survey: frequency and duration of voltage sags and surges at industrial sites," *IEEE Trans. on Industry Applications*, vol. 34, no. 5, pp. 904-910, September/October 1998.

[3] C. J. Melhorn, M. F. McGranaghan, "Interpretation and analysis of power quality measurements," *IEEE Trans. on Industry Applications*, vol. 31, no. 6, pp. 1363-1370, November/December 1995.

[4] EPRI, "The cost of power disturbances to industrial and digital economy companies," EPRI Executive Summary 1006274, 3412 Hillview Avenue, Palo Alto, CA. 94304.

[5] D. Sabin, "An assessment of distribution system power quality, volume. 2: statistical summary report," 3412 Hillview Avenue, Palo Alto, CA. 94304. EPRI Final Report TR-106294-V2, May 1996.

[6] J. L. Duran-Gomez, P. N. Enjeti, and B. O. Woo, "Effect of voltage sags on adjustable speed drives – A critical evaluation and approach to improve its performance," in *Proc. of 14th Annual Applied Power Electronics Conference and Exposition (APEC)*, vol. 2, pp. 774-780, March 14-18, 1999.

[7] M. H. J. Bollen, "Voltage sags in three-phase systems," *IEEE Power Engineering Review*, pp. 8-15, September 2001.

[8] EPRI Power Electronics Applications Center, "Input performance of ASDs during supply voltage unbalance," Power Quality Testing Network PQTN Brief no. 28, 1996.

[9] J. P. G. de Abreu, A. E. Emanuel, "Induction motor thermal aging caused by voltage distortion and imbalance: Loss of useful life and its estimated cost," *IEEE Trans. on Industry Applications*, vol. 38, no. 1, pp. 12-20, January/February 2000.

[10] K. Lee, T. M. Jahns, W. E. Berkopec, T. A. Lipo, "Closed-form analysis of adjustable speed drive performance under input voltage unbalance and sag conditions", in *Proc. of 35th IEEE Power Electronics Specialists Conference (PESC'04)*, pp. 469-475, Aachen, Germany, June 2004.

[11] "IEEE recommended practice for electric power distribution for industrial plants", IEEE Standard 141-1993, 1993.

[12] K. Lee, G. Venkataramanan, T. M. Jahns, "Design-oriented Analysis of dc bus dynamics in adjustable speed drives under input voltage unbalance and sag conditions", in *Proc. of 35th IEEE Power Electronics Specialists Conference (PESC'04)*, pp. 1675-1681, Aachen, Germany, June 2004.

[13] W. T. McLyman, *Transformer and inductor design handbook*, Third ed., Marcel Dekker, Inc., New York, 2004.